Finite-size effects on the dynamics of the zero-range process

Shamik Gupta,[1] Mustansir Barma,[1] and Satya N. Majumdar[2]
[1] *Department of Theoretical Physics, Tata Institute of Fundamental Research, Homi Bhabha Road, Mumbai, India*
[2] *Laboratoire de Physique Théorique et Modèles Statistiques, Université Paris-Sud, Orsay, France*
(Dated: December 12, 2007)

We study finite-size effects on the dynamics of a one-dimensional zero-range process which shows a phase transition from a low-density disordered phase to a high-density condensed phase. The current fluctuations in the steady state show striking differences in the two phases. In the disordered phase, the variance of the integrated current shows damped oscillations in time due to the motion of fluctuations around the ring as a dissipating kinematic wave. In the condensed phase, this wave cannot propagate through the condensate, and the dynamics is dominated by the long-time relocation of the condensate from site to site.

PACS numbers: 05.70.Ln, 02.50.Ey, 05.40.-a, 64.60.-i

The dynamics of fluctuations in simple nonequilibrium steady states of interacting particle systems has been studied extensively in recent years, and a fairly good understanding of the physical processes involved has been achieved in infinite systems [1]. Studies of these fluctuations in a finite system show a strong imprint of the nonequilibrium character, which combines with size effects to bring in interesting dynamical phenomena [2]. Many of these systems often exhibit a nonequilibrium phase transition in the steady state, from a disordered to an ordered phase, as one tunes an external parameter such as the density. This raises the natural question: How is the dynamics of fluctuations in the steady state affected as the system passes through a nonequilibrium phase transition? In this paper, we address this issue within the ambit of a paradigmatic model, the zero-range process (ZRP) [3, 4], and show that there are strong differences in the dynamical properties arising from very different physical processes in the two phases.

The ZRP involves biased hopping of particles on a periodic lattice with a rate that depends on the occupancy at the departure site. At long times, the system reaches a nonequilibrium steady state. For certain classes of the hop rates, as the particle density crosses a critical threshold, there is a continuous phase transition from a disordered phase with uniform average density to a condensed phase where a finite fraction of particles (the "condensate") accumulates on a single site [4]. The ZRP applies to a wide variety of physical systems ranging from traffic flow [5] to shaken granular gases [6]; in addition, it was invoked to provide a criterion for phase separation in one-dimensional driven systems [7].

Recent work on the ZRP has dealt with the relaxation of an initial homogeneous density distribution toward the condensed phase [8]. By contrast, here we are interested in the dynamics of density fluctuations in the *steady state* in both the disordered and the condensed phases. We explore the dynamics by monitoring the variance of the integrated particle current in Monte Carlo simulations and supplement our findings by analyzing the survival probability distribution of the largest mass in the system. The relevant time scales in the behavior of fluctuations in the two phases and the physical effects underlying them are summarized below.

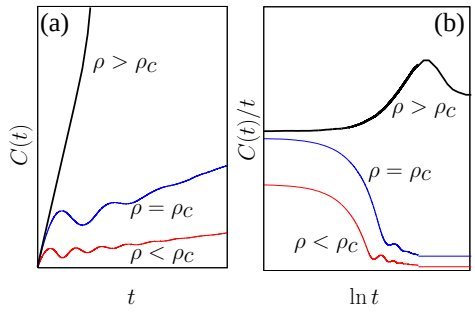

FIG. 1: (Color online) (a) Schematic plot of the integrated current fluctuations $C(t)$ across a bond in the steady state of the ZRP as a function of time t in the disordered phase ($\rho < \rho_c$), at the critical point ($\rho = \rho_c$), and in the condensed phase ($\rho > \rho_c$). (b) Schematic plot of $C(t)/t$ as a function of t in all the phases.

In Fig. 1, we show schematically the behavior of the variance of the integrated current as a function of time in different phases. In all the phases, at short times, the integrated current is Poisson distributed, implying that the variance grows linearly in time, a behavior which holds for all times in an infinite system. In a finite system, in the disordered phase and at criticality, the variance shows oscillations at times proportional to the system size L. This results from kinematic waves transporting density fluctuations around the system with a well-defined speed. At longer times ($\sim L^{3/2}$), the wave decays, and then the variance increases linearly with time with a small slope that decreases with increasing system size. In the condensed phase, however, the kinematic wave cannot pass through the condensate; thus, fluctuations do not circulate around. The initial linear behavior continues until, after a characteristic time which grows as a power of the

system size, the condensate relocates itself. This results in the variance showing a linear rise in time with a much larger slope than at early times. Subsequently, after the condensate has relocated to another site, the slope of the linear rise slowly approaches a size-dependent constant.

We now turn to a derivation of these properties. The ZRP involves N particles of unit mass on a ring of size L with arbitrary occupancy allowed at any site. A particle hops out of a randomly selected site i with occupancy n_i with a specified rate $u(n_i)$, and goes to site $(i+1)$. In the thermodynamic limit $N \to \infty, L \to \infty$ at a fixed density $\rho = N/L$, the probability $P(\mathbf{C})$ of a configuration $\mathbf{C} \equiv \{n_i\}$ in the steady state, in the grand canonical ensemble, is given by [4]

$$P(\mathbf{C}) = \frac{1}{Z} \prod_{i=1}^{L} v^{n_i} f(n_i),$$

$$f(n) = \begin{cases} \left(\prod_{l=1}^{n} u(l) \right)^{-1} & \text{if } n > 0, \\ 1 & \text{if } n = 0. \end{cases} \qquad (1)$$

Here, Z is the partition function and v is the fugacity. The average mass at a site equals $vF'(v)/F(v)$, where $F(v) = 1 + \sum_{n=1}^{\infty} v^n f(n)$. Particle conservation gives a relation between ρ and v, namely, $\rho = vF'(v)/F(v)$. The fugacity has the maximum value $v_{\max} = u(\infty)$, given by the radius of convergence of the infinite series $F(v)$. The ZRP can be mapped to a generalization of the asymmetric simple exclusion process (ASEP) by interpreting the ZRP sites as particles in the ASEP, while the particles at a ZRP site become holes preceding the corresponding ASEP particle [4]. The hop rate $u(n)$ for an ASEP particle, now a function of the headway to the next particle, induces a long-ranged particle hopping.

Here, we consider the hop rate $u(n) = 1 + b/n$ with $b > 2$ for which the system undergoes a nonequilibrium phase transition [4]. As ρ crosses the critical value $\rho_c = 1/(b-2)$ [8], a low-density disordered phase with mass of $O(1)$ at each site evolves to a high-density condensed phase where a macroscopic collection of particles of average mass $(\rho - \rho_c)L$ condenses onto a randomly selected site, while the remaining sites have the average mass ρ_c.

In the steady state, the mean current of particles between every pair of neighboring sites is the same. In the thermodynamic limit, the mean current is $J = \sum_{n=1}^{\infty} u(n) v^n f(n)/F(v) = v$. It increases with the density ρ, attaining its maximum value $v_{\max} = u(\infty) = 1$ at ρ_c, and remaining pinned to this value in the condensed phase. To address the dynamics of density fluctuations, we examine the fluctuations in the integrated particle current across any bond in the steady state. The large deviation function of the integrated current has been studied for the ZRP with open boundaries in [9]. For our purpose, we monitor the variance $C(i,t)$ of the integrated current $H(i,t)$ which counts the total number of particles crossing the bond $(i, i+1)$ in time t. Thus, we have

$$C(i,t) \equiv \langle H^2(i,t) \rangle - \langle H(i,t) \rangle^2. \qquad (2)$$

In the equivalent ASEP, $C(i,t)$ is a measure of tagged particle correlations, being given by the variance of the ith tagged particle around its average displacement in time t. In simulations, we monitor $C(t) = \sum_{i=1}^{L} C(i,t)/L$ and find that it shows strong differences in behavior in the disordered and the condensed phases, reflecting very different underlying physical processes in the two phases.

Disordered phase. $C(t)$ in this phase behaves similarly to the tagged particle correlation in the ordinary ASEP, studied recently [2]. As discussed below, there are two scales $T_1 \sim L$, set by the circulation time of a kinematic wave of density fluctuations, and $T_2 \sim L^{3/2}$, given by the time taken by this wave to decay.

(i) $t \ll T_1$. Here, $C(t)$ grows linearly in time: $C(t) = vt$. This follows from the result that, in this time regime, $H(i,t)$ is Poisson distributed with intensity v over all bonds $(i, i+1)$. The population at a ZRP site undergoes a time-reversible birth-death process where a birth (particle input) occurs with rate v, while a population of n particles undergoes a death with rate $u(n)$. For a reversible birth-death process with Poisson inputs, Burke's theorem implies an identical Poisson distribution of outputs [10]. Noting that the output from one site forms the input to the next site then implies the result [11].

(ii) $T_1 \ll t \ll T_2$. In this regime, $C(t)$ oscillates as a function of time. In a driven system with homogeneous density ρ and a density-dependent current $J(\rho)$, density fluctuations are transported as a kinematic wave with speed $v_K = \partial J/\partial \rho$ [12]. This wave is dissipated over a time scale $\sim L^z$, where z is the dynamic exponent of the system. For the ZRP, z takes on the Kardar-Parisi-Zhang (KPZ) value of 3/2 [13]. Since $z > 1$, fluctuations circulate several times around a periodic system before getting dissipated, and revisit every site after a time L/v_K. This makes the variance oscillate in time with this period. A measure of the growth of dissipation in time is given by the lower envelope of the oscillations, which behaves as $t^{2\beta}$ where $\beta = \beta_{\rm KPZ} = 1/3$ [13].

(iii) $t \gg T_2$. The time scale T_2 marks the dissipation time of an initial density profile. For times $t \gg T_2$, the variance grows diffusively: $C(t) \sim D(L)t$. Matching this behavior at T_2 with that in (ii) above gives $D(L) \sim L^{-1/2}$, as for the ordinary ASEP [14].

Critical point. At the critical density ρ_c, the variance behaves differently for values of $b \leq 3$ and $b > 3$. For $b \leq 3$, there is no moving kinematic wave [8]. Hence, the integrated current is Poisson distributed with intensity $v_{\max} = 1$, implying that the variance continues to grow linearly with slope 1. For $b > 3$, however, the kinematic wave speed is nonzero and the Poisson distribution for the integrated current is expected to hold for times smaller

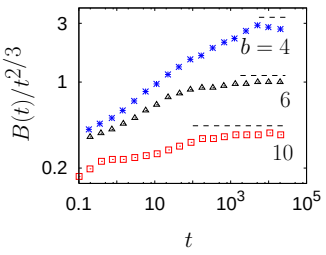

FIG. 2: (Color online) Monte Carlo (MC) simulation results for $B(t)/t^{2/3}$ as a function of time t for different b's at $\rho_c = 1/(b-2)$. The system size is $L = 16\,384$. The dashed lines show the asymptotic $t^{2/3}$ approach.

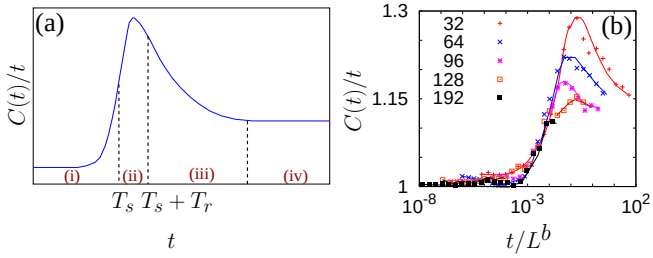

FIG. 3: (Color online) (a) Schematic plot of $C(t)/t$ as a function of time t in the condensed phase. The various regimes (see text) are also marked. (b) Scaling of $C(t)/t$ with t/L^b for $b = 3$ in the condensed phase ($\rho = 4$). Various system sizes L considered are marked in the figure. The data points, obtained from MC simulations, are connected by smooth curves.

than the return time of the kinematic wave. At criticality, the largest mass in the system scales as $\sim L^{1/(b-1)}$ [15] and is insufficient to block the circulation of the kinematic wave around the system. $C(t)$ oscillates in time as for $\rho < \rho_c$, with return time T_1 and decay time T_2 of the kinematic wave. To find the exponent β at criticality, we monitored the variance $B(t)$ of the integrated current by starting from an arbitrary but *fixed* initial configuration, drawn from the stationary ensemble [16]. $B(t)$ grows asymptotically as $t^{2\beta}$ for $t \ll L^{3/2}$ [2]. We find that β at criticality has the KPZ value of 1/3, independent of b (Fig. 2).

Condensed phase. For $\rho > \rho_c$, a finite fraction of the total mass (the condensate) resides on one site for the characteristic survival time $T_s \sim (\rho - \rho_c)^{b+1} L^b$ [17]. It then relocates to another site over the relocation time scale $T_r \sim (\rho - \rho_c)^2 L^2$, as discussed below. The behavior of $C(t)$ in this phase is best depicted by plotting $C(t)/t$ as a function of time, as shown schematically in Fig. 3(a), where the various regimes are also marked.

(i) $t \ll T_s$: Here, $C(t)/t$ equals 1, with a mild upward deviation for longer times. (ii) $t \sim T_s$: In this regime, $C(t)/t$ rises rapidly in time. (iii) $t \gtrsim T_s + T_r$: Here, $C(t)/t$ falls slowly in time. (iv) $t \gg T_s + T_r$: Here, $C(t)/t$ begins

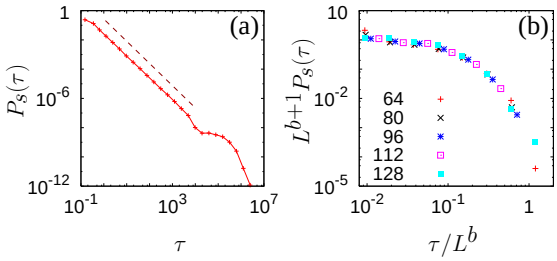

FIG. 4: (Color online) (a) Survival probability distribution $P_s(\tau)$ of the largest mass in the condensed phase. The system size $L = 128$, the parameter $b = 3$, while $\rho = 4$. The dashed line is a guide to the eye for the part of $P_s(\tau)$ behaving as $\tau^{-3/2}$. (b) Scaling of the bump in $P_s(\tau)$. The data are obtained from MC simulations.

to approach a size-dependent constant, as predicted by a simple model described later in this paper. Features (ii), (iii), and (iv) result from enhanced fluctuations due to the condensate relocation. To understand this, we need to first discuss the relocation dynamics.

The condensate relocation occurs through exchange of particles between two sites. On monitoring the time evolution of the largest and the second largest mass in simulation, the following picture emerges. Let $M(t)$ denote the largest mass in the steady state at time t. $M(t)$ has the average value $M_0 \equiv \langle M(t) \rangle = (\rho - \rho_c)L$, with fluctuations ΔM_0 which scale as $L^{1/2}$ for $b > 3$, and as $L^{1/(b-1)}$ for $2 < b < 3$ [18]. These fluctuations may build up in time, and over the time scale T_s, the largest mass fluctuates to $\sim M_0/2$, while a mass $\sim M_0/2$ also builds up at another site. Subsequent to this, two sites with mass $\sim M_0/2$ exchange particles between themselves resulting in relatively rapid alternating relocations of the largest mass from one site to the other. The difference of masses on these two sites performs an unbiased random walk in time until fluctuations populate one of the sites to $\sim M_0$ at the expense of the other, which happens over the time scale $T_r \sim (\rho - \rho_c)^2 L^2$.

Figure 4(a) shows the Monte Carlo results for the survival probability distribution $P_s(\tau)$ of the largest mass, obtained by computing the distribution of the time interval between successive relocations. $P_s(\tau)$ has two parts, (i) a power law part $\sim \tau^{-3/2}$ and (ii) another part, which corresponds to the bump in Fig. 4(a), and has the scaling form $(\rho - \rho_c)^{-(b+2)} L^{-(b+1)} f(\tau/T_s)$, as shown in Fig. 4(b). The prefactor comes from the normalization of $P_s(\tau)$ to unity, with the cutoff for the $\tau^{-3/2}$ part taken to scale as T_r. The power law part holds for times when the two sites with mass $\sim M_0/2$ compete to hold the largest mass. The random walk argument of the preceding paragraph predicts a $\tau^{-3/2}$ decay, since $P_s(\tau)$ then stands for the probability for the random walker to cross the origin for the first time. The second part in $P_s(\tau)$ arises from the relatively long time for which the condensate is

stationary on one site.

We now explain the behavior of $C(t)/t$ in the different regimes seen in Fig. 3(a). The condensate is stationary on one site for a long time τ_1, which is a random interval distributed as $p(\tau_1) \sim (\rho - \rho_c)^{-(b+2)} L^{-(b+1)} f(\tau_1/T_s)$, with the characteristic survival time T_s. In regime (i), when $t \ll T_s$, the condensate is stationary and acts as a reservoir for fluctuations, preventing their transport around the system as a kinematic wave. As a result, Burke's theorem is valid over this time scale and the integrated current is Poisson distributed with intensity $v_{\max} = 1$, implying $C(t)/t = 1$. When $t \sim T_s$, the condensate starts to move from one site to another by transferring its mass across the intervening bonds. As a result, these bonds pick up enhanced fluctuations [$\propto (\Delta M_0)^2$] in the integrated current over the relocation time interval τ_2, which is a random variable with the characteristic time T_r. These enhanced fluctuations lead to the rise in $C(t)/t$ as a function of t in regime (ii). The collapse of the rise times seen in the scaling plot of Fig. 3(b) confirms this picture. In regime (iii), after $t \sim T_s + T_r$, the condensate has completed relocating, so current fluctuations revert to Burke-like behavior, resulting in the fall of $C(t)/t$ in time. The slow fall in regime (iii) arises from the wide distribution of the time τ_2, and further relocations. To predict the behavior in regime (iv), where $t \gg T_s + T_r$, we construct below a simple relocation model (RM) that describes the effect of condensate relocation on the long-time behavior of current fluctuations.

Figure 5 shows schematically the instantaneous current $j(i,t)$ across the bond $(i, i+1)$ as a function of time. In a given history, let K be the number of condensate relocations in a fixed time t. Here, K is a random variable with mean given approximately by $\langle K \rangle \approx t/(DT_s + BT_r)$, where B and D are constants, independent of the density and the system size. At the kth relocation of the condensate ($k = 1, 2, \ldots, K$), let $\widetilde{M}_k$ denote the amount of mass transferred across the bond $(i, i+1)$ over the interval τ_2. The random variable $\widetilde{M}_k$ has an average M_0 and variance ΔM_0. The integrated current $H(i,t)$ is given approximately as $H(i,t) \approx \sum_{k=1}^{K} \widetilde{M}_k + \int_0^{t-KBT_r} dt' j(i,t')$. For $b > 3$, on computing the variance of the integrated current, we get $C(t) \approx GL\langle K \rangle + (t - \langle K \rangle BT_r)$, where G is a constant. On substituting for $\langle K \rangle$ and neglecting the time scale $T_r \sim (\rho - \rho_c)^2 L^2$ in comparison to $T_s \sim (\rho - \rho_c)^{b+1} L^b$, we obtain the asymptotic behavior

$$C(t) \sim [L^{-\theta} (\rho - \rho_c)^{-(b+1)} + 1] t, \qquad (3)$$

with $\theta = b - 1$ for $b > 3$. For b between 2 and 3, we find that $\theta = (b^2 - b - 2)/(b - 1)$. Thus, the RM predicts that, for all values of b, at long times $t \gg T_s + T_r$ [regime (iv)], $C(t)/t$ approaches a size-dependent constant which scales down with the system size. This long-time regime (iv) could not be accessed in simulations for the system sizes shown in Fig. 3(b), but we confirmed its existence for smaller systems.

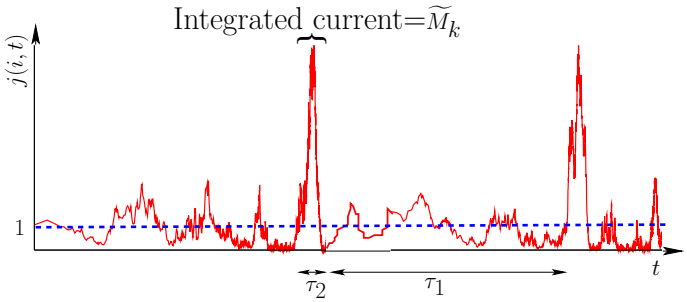

FIG. 5: (Color online) Schematic plot of the instantaneous current $j(i,t)$ across the bond $(i, i+1)$ at time t as a function of time. The random variable τ_1 is the time for which the condensate is stationary on a site, while the random variable τ_2 stands for the relocation time of the condensate. $\widetilde{M}_k$ is the integrated current over time τ_2, arising from the kth relocation of the condensate across the bond $(i, i+1)$.

In summary, we addressed the dynamics of steady state fluctuations of a zero-range process which undergoes a nonequilibrium phase transition from a disordered to a condensed phase. Different dynamical properties emerge in the two phases. In the disordered phase, fluctuations move around the system as a kinematic wave. Such a wave, though present in the bulk, cannot circulate around in the condensed phase because the condensate subsumes fluctuations. The dynamics is governed by the condensate relocation through a slower process of transfer of particles from site to site, contributing enhanced fluctuations to the particle current across the intervening bonds.

M.B. and S.N.M. acknowledge the Indo-French Centre for the Promotion of Advanced Research (IFCPAR) for support under Project No. 3404-2.

[1] R. Stinchcombe, Adv. Phys. **50**, 431 (2001); G. M. Schütz, in *Phase Transitions and Critical Phenomena*, edited by C. Domb and J. L. Lebowitz (Academic, London, 2001), Vol. 19.
[2] S. Gupta, S. N. Majumdar, C. Godrèche, and M. Barma, Phys. Rev. E **76**, 021112 (2007).
[3] F. Spitzer, Adv. Math. **5**, 246 (1970).
[4] M. R. Evans and T. Hanney, J. Phys. A **38**, R195 (2005).
[5] D. Chowdhury, L. Santen, and A. Schadschneider, Phys. Rep. **329**, 199 (2000).
[6] J. Török, Physica A **355**, 374 (2005).
[7] Y. Kafri, E. Levine, D. Mukamel, G. M. Schütz, and J. Török, Phys. Rev. Lett. **89**, 035702 (2002).
[8] S. Großkinsky, G. M. Schütz, and H. Spohn, J. Stat. Phys. **113**, 389 (2003); C. Godrèche, J. Phys. A **36**, 6313 (2003).
[9] R. J. Harris, A. Rákos, and G. M. Schütz, J. Stat. Mech.: Theory Exp. 2005, P08003.
[10] P. J. Burke, Oper. Res. **4**, 699 (1956); E. Reich, Ann.

Math. Stat. **28**, 768 (1957).
[11] We are grateful to J. Lebowitz and E. Speer for pointing out the applicability of the Burke's theorem to the ZRP.
[12] M. J. Lighthill and G. B. Whitham, Proc. R. Soc. London, Ser. A **229**, 281 (1955).
[13] M. Kardar, G. Parisi, and Y. C. Zhang, Phys. Rev. Lett. **56**, 889 (1986).
[14] B. Derrida, M. R. Evans, and D. Mukamel, J. Phys. A **26**, 4911 (1993); B. Derrida and K. Mallick, *ibid.* **30**, 1031 (1997).
[15] This follows from applying extreme value statistics to the power law distribution of mass, $p(n) \sim n^{-b}$.
[16] H. van Beijeren, J. Stat. Phys. **63**, 47 (1991).
[17] C. Godrèche and J. M. Luck, J. Phys. A **38**, 7215 (2005).
[18] S. N. Majumdar, M. R. Evans, and R. K. P. Zia, Phys. Rev. Lett. **94**, 180601 (2005).